Harmonic spectra bandwidth broadening with a new polarization gating

Jing Miao (苗 境)[1], Pengfei Wei (尉鹏飞)[2], Zhinan Zeng (曾志男)[1*], Chuang Li (李 闯)[1], Xiaochun Ge (葛晓春)[1], Ruxin Li (李儒新)[1,3], and Zhizhan Xu (徐至展)[1,3]

[1]*State Key Laboratory of High Field Laser Physics, Shanghai Institute of Optics and Fine Mechanics, Chinese Academy of Sciences, Shanghai 201800, China*

[2]*College of Physics and Electronic Information Engineering, Wenzhou University, Wenzhou 325035, China*

[3]*School of Physical Science and Technology, Shanghai Tech University, Shanghai 200031, China*

[*]*Corresponding author: zhinan_zeng@siom.ac.cn*

Received October 25, 2013; accepted March 5, 2014; posted online April 4, 2014

A new polarization gating is demonstrated by our principle-of-proof experiment, which is theoretically proposed to generate the isolated or double attosecond pulses with the multi-cycle driving laser pulse in the previous work [Optics Express. 20, 5196 (2012)]. In the experiment, the polarization gating is formed by two orthogonally-polarized linearly chirped multi-cycle laser pulses, and the spectral bandwidths of the harmonics are broadened by more than two times, which agree with the previous theoretical work.

OCIS codes: 020.1335, 020.2649, 190.2620.
doi: 10.3788/COL201412.040201.

Extreme nonlinear optical process in the interaction of an ultrashort laser pulse with atoms or molecules has been widely investigated for studying the electron dynamics[1−6], teraherhz tomographic imaging[7,8], producing the attosecond XUV pulse[8] and the others in experiment. The process of the HHG can be controlled through modifying the quantum path of the ionization electron, such as controlling the chirp[9], the two-color laser field[10], and the polarization gating[11−13]. The HHG process has been described with the three-step model[14] which includes the ionization, the acceleration and the recombination. This model shows that we can control the three steps by using the special laser fields to change the acceleration or recombination and to achieve particular high-order harmonic spectrum. For example, in the two-color experiment, the period of the recombination events is the full optical cycle instead of the half-cycle in the case of one-color field[10]. It also has been reported that using the combination of a chirped laser and a static field can extend the cutoff and increase the maximum harmonic photon energy[15,16].

In general, the electric field of the polarization gating has been generated by combining two counter rotating circularly polarized laser pulses[11]. The modulation of the ellipticity in this polarization gating electric field results in that the field can generate a high-order harmonics only when the ellipticity is enough smaller . We have also proposed a new polarization gating scheme which can generate two coherent at to second pulses with a tunable delay[17]. In this letter, we perform a principle-of-proof experiment for this new polarization gating scheme and demonstrate that the spectral bandwidth of harmonics can be controlled by the delay of two orthogonally-polarized linearly chirped multi-cycle laser pulses. We also calculate the HHG using the Lewenstein model[18] with this kind of laser field and find almost the same harmonic broadening.

The harmonics are generated from the argon gas by using the experiment setup shown in Fig. 1. In this experiment, we use the 800-nm laser field with a positive chirp. The value of this positive chirp can be adjusted by the chirped mirrors in the laser system. This positive chirp pulse is splited into two pulses by the first beam splitter (BS). Then a quartz plant (QP) and a glass (G) are used to make one pulse orthogonalizing the other and having a negative chirp. Two pulses are both broadened to be almost 70 fs by adjusting the chirped mirrors and the thickness of the glass (G). The wedges are used for changing the delay between these two pulses.

The orthogonally polarized chirped laser pulses, with the each pulse energy of 0.75 mJ, are focused to an argon gas jet to generate the high-order harmonics. The harmonics pass through an Al filter and are sent into a homemade XUV spectrometer, and then are detected by the X-ray CCD.

In this letter, we mainly investigate the feature of the harmonic spectrum changed by the delay between the two orthogonally polarized linearly chirped pulses. Figure 2 shows the typical harmonic spectra obtained in this experiment, with the relative delays of 0 (a) and

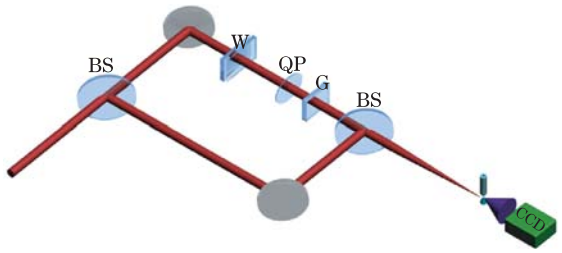

Fig. 1. Experimental setup for the orthogonally-polarized chirped laser fields, consisting of two beam splitters (BS), two mirrors, two parallel wedges (W), and a glass (G). A gas jet and a CCD are also shown in the figure for generation and detection of the high order harmonics.

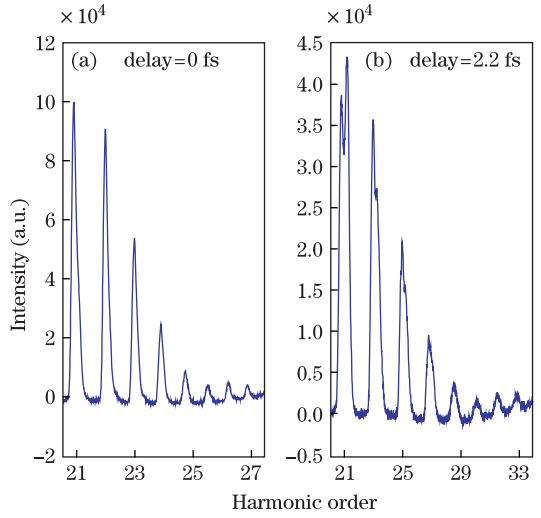

Fig. 2. Typical harmonic spectra for two different time delays. The time delay is a relative delay between two orthogonally polarized chirped pulses, which is adjusted by the wedge.

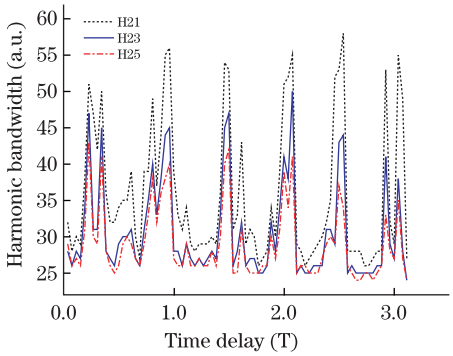

Fig. 3. Spectral bandwidth of each harmonic as a function of the time delay between the two orthogonally polarized chirped pulses. The maximum bandwidth of the 21st harmonic can be broadened to 55, which is more than two times of the minimum bandwidth of the 21st harmonic.

2.2 fs (b) (the time delay is set to the relative time delay). In the case of 0-fs delay, a well-resolved harmonic spectrum can be observed and only one peak exists in each harmonic shown in Fig. 2(a). But for the case of 2.2-fs delay, the harmonic is obviously broadened and the split can be seen in some harmonics. The broadening of the harmonics is shown in Fig. 3. The black dashed line in Fig. 3 represents the bandwidth of the 21st harmonic as a function of the time delay between the two pulses. The bandwidth can be broadened by more than two times. We calculate the HHG with the Lewenstein model[18] to investigate this process, taking into account the parameters used in the experiment. The detail can be found in Ref. [17]. With the simulation, we can get the HHG spectrum as a function of the delay between the two orthogonally laser fields. In this simulation, the laser intensity is 1×10^{14} W/cm^2 which could make the cutoff almost the same with experimental results. The results of 21st, 23rd and 25th harmonics are shown in Fig. 4(a) in detail. The simulation results agree with the experimental results with the same period and broadening. But there is a little different: an obvious interference can be seen in the calculation result around the time delays of 0.2 and 1.5 fs, but it cannot be found in the measured harmonic spectrum around these delays which may be eliminated by the propagation effect in the experiment. In Fig. 4(b), the bandwidth of the 21st harmonic shows changing with the time delay between the two orthogonally laser fields which agrees with the results shown in Fig. 3.

A deeper insight of the physical mechanism can be obtained by using the time frequency analysis for the high-order harmonic spectra. Different curves in Fig. 5(a) show the 21st harmonic with the different time delays. The time-frequency distributions of the three time delays are shown in Figs. 5(b)-(d). As shown in Figs. 5(a) and 5(b), the bandwidth of the 21st harmonic is about 180 (arb. unit) when the time delay is 0.2 fs, while the time-frequency distribution shows that the time window for the generation of the 21st harmonic is divided into two parts and each time window is about 4 T (T is the optical

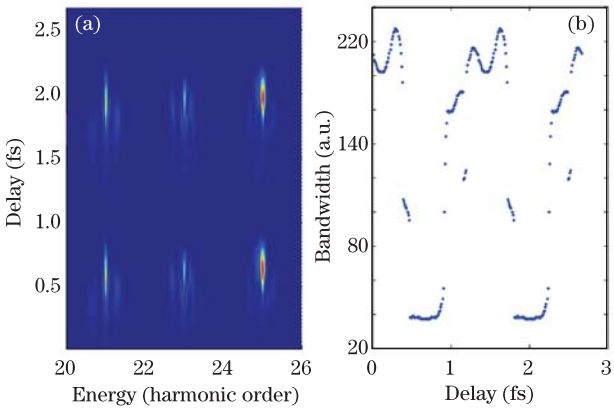

Fig. 4. (a) HHG spectra versus time delay between the two orthogonally laser fields. A 24-fs initial laser pulse is used in the calculation. We choose N=3 to broaden the pulse width to 72 fs, which is close to the pulse width in the experiment. (b) Spectral bandwidth of the 21st harmonic.

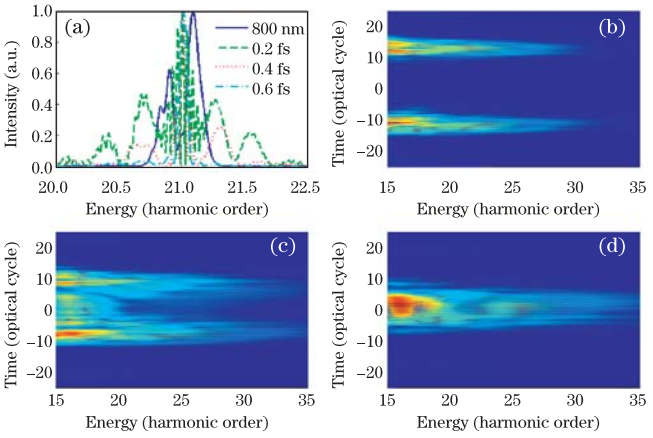

Fig. 5. (Color online) (a) The 21st harmonic spectra produced from the combined fields with the time delay of 0.2 fs (green dashed line), 0.4 fs (red line) and 0.6 fs (cyan line). The blue line shows the 21th harmonic spectra under the only 800-nm electric field. (b)−(d) The time-frequency distributions of the HHG of different time delays (0.2, 0.4, and 0.6 fs) shown in (a), respectively.

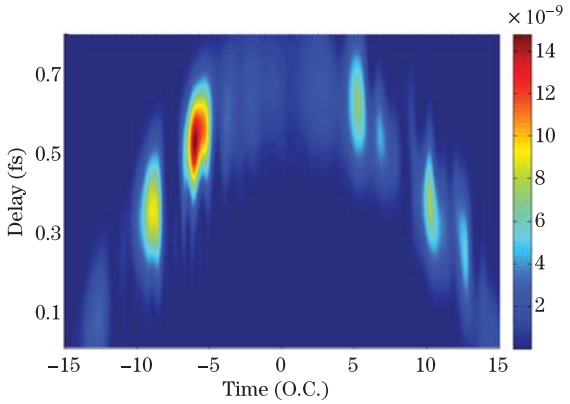

Fig. 6. Temporal profiles of the 21st harmonic as a function of the time delay between two pulses. When the delay is shorter than 0.4 fs, the duration of the 21st harmonic in one part can be about 1 T.

cycle of the 800-nm pulse). In the case of 0.4 fs (Fig. 5(c)) and 0.6 fs (Fig. 5(d)) time delays, the bandwidth of the 21st harmonic are about 100 a.u. and 40 a.u., while the time windows for the generation of the 21st harmonic are about 20 T and 8 T, respectively. In Fig. 5(a), the spectra show an obvious interference at some delays. By comparing with the time-frequency distributions of the different time delays, we find that the harmonic interference come from the time interval between the harmonics generated in the different times, and this is corresponding to the statement in our early work in Ref. [17]. The temporal profiles of the 21st harmonic as a function of the time delay are shown in Fig. 6. The shortest emisstion of the 21st harmonic can be about 1 T.

In conclusion, we experimentally demonstrate that the harmonic bandwidth can be broadened by a new polarization gating formed by two orthogonally-polarized linearly chirped multi-cycle laser pulses, which is theoretically proposed by in the Ref. [17]. This method can be used to generate the isolated attosecond pulse with multi-cycle driving laser pulses if using a longer wavelength laser field.

This work was supported by the National Natural Science Foundation of China (Nos. 11127901, 61221064, 11134010, 11222439, and 61108012), the National "973" Project of China (No. 2011CB808103), the Postdoctoral Science Foundation of China (Nos. 2012T50420 and 2012M520941), the Postdoctoral Scientific Research Program of Shanghai (No. 12R21416600), and the Open Fund of the State Key Laboratory of High Field Laser Physics.

References

1. J. Zhao and M. Lein, Phys. Rev. Lett. **111,** 043901 (2013).
2. O. Raz, O. Schwartz, D. Austin, A. S. Wyatt, A. Schiavi, O. Smirnova, B. Nadler, I. A. Walmsley, D. Oron, and N. Dudovich, Phys. Rev. Lett. **107,** 133902 (2011).
3. S. Gilbertson, M. Chini, X. Feng, S. Khan, Y. Wu, and Z. Chang, Phys. Rev. Lett. **105,** 263003 (2010).
4. Y. Wang, Z. Sun, X. Zhang, J. Xiao, L. Deng, W. Zhang, Z. Wang, and Z. Zeng, Chin. Opt. Lett. **4,** 49 (2006).
5. J. Mauritsson, T. Remetter, M. Swoboda, K. Klüder, A. L'Huillier, K. J. Schafer, O. Ghafur, F. Kelkensberg, W. Siu, P. Johnsson, M. J. J. Vrakking, I. Znakovskaya, T. Uphues, S. Zherebtsov, M. F. Kling, F. Lépine, E. Benedetti, F. Ferrari, G. Sansone, and M. Nisoli, Phys. Rev. Lett. **105,** 053001 (2010).
6. W. Cheng, S. Zhang, T. Jia, J. Ma, D. Feng, and Z. Sun, Chin. Opt. Lett. **11,** 041903 (2013).
7. T. Wang, S. Yuan, Y. Chen, and S. Chin, Chin. Opt. Lett. **11,** 011401 (2013).
8. Z. Zeng, Y. Cheng, X. Song, R. Li, and Z. Xu, Phys. Rev. Lett. **98,** 203901 (2007).
9. J. Xiao, Z. Sun, X. Zhang, Y. Wang, W. Zhang, Z. Wang, R. Li, and Z. Xu, J. Opt. Soc. Am. B **23,** 771 (2006).
10. Z. Zeng, Y. Cheng, X. Song, R. Li, and Z. Xu, Phys. Rev. Lett. **98,** 203901 (2007).
11. Z. Chang, Phys. Rev. A **70,** 043802 (2004).
12. S. D. Khan, Y. Cheng, M. Möller, K. Zhao, B. Zhao, M. Chini, G. G. Paulus, and Z. Chang, Appl. Phys. Lett. **99,** 161106 (2011).
13. Y. Zheng, H. Xiong, Z. Zeng, Y. Huo, Z. Wang, X. Ge, R. Li, and Z. Xu, Chin. Opt. Lett. **5,** 118 (2007).
14. P. B. Corkum, N. H. Burnett, and M. Y. Ivanov, Opt. Lett. **19,** 1870 (1994).
15. Y. Xiang, Y. Niu, and S. Gong, Phys. Rev. A **79,** 053419 (2009).
16. H. Du, L. Luo, X. Wang, and B. Hu, Opt. Express **20,** 9713 (2012).
17. J. Miao, Z. Zeng, P. Liu, Y. Zheng, R. Li, Z. Xu, V. T.Platonenko, and V. V. Strelkov, Opt. Express **20,** 5196 (2012).
18. M. Lewenstein, Ph. Balcou, M. Yu. Ivanov, Anne L'Huillier, and P. B. Corkum, Phys. Rev. A **49,** 2117 (1994).